Article

Promoting Lignin Depolymerization and Restraining the Condensation via an Oxidation-Hydrogenation Strategy

Chaofeng Zhang, Hongji Li, Jianmin Lu, Xiaochen Zhang,
Katherine E MacArthur, Marc Heggen, and Feng Wang

Just Accepted

Promoting Lignin Depolymerization and Restraining the Condensation *via* an Oxidation-Hydrogenation Strategy

Chaofeng Zhang,[a] Hongji Li,[a,b] Jianmin Lu,[a] Xiaochen Zhang,[a] Katherine E. MacArthur,[c] Marc Heggen[c] and Feng Wang[a]*

[a] State Key Laboratory of Catalysis, Dalian National Laboratory for Clean Energy, Dalian Institute of Chemical Physics, Chinese Academy of Sciences, Dalian 116023 (China)

[b] University of Chinese Academy of Sciences, Beijing 100049 (China)

[c] Ernst Ruska Centre for Microscopy and Spectroscopy with Electrons and Peter Grünberg Institute, Forschungszentrum Juelich GmbH, Juelich 52425 (Germany)
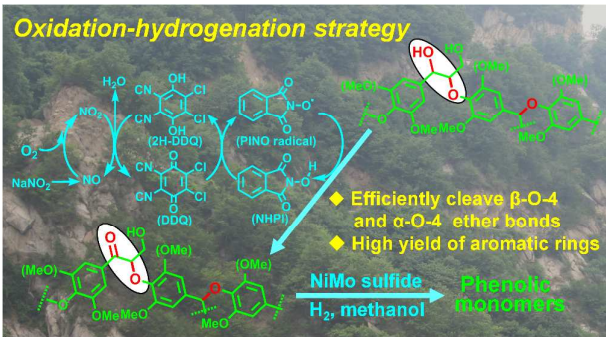
ABSTRACT:

For lignin valorization, simultaneously achieving the efficient cleavage of ether bonds and restraining the condensation of the formed fragments represents a challenge thus far. Herein, we report a two-step oxidation-hydrogenation strategy to achieve this goal. In the oxidation step, the O_2/$NaNO_2$/DDQ/NHPI system selectively oxidizes $C_\alpha H–OH$ to $C_\alpha=O$ within β-O-4 structure. In the subsequent hydrogenation step, the α-O-4 and the pre-oxidized β-O-4 structures are further hydrogenated over a NiMo sulfide catalyst, leading to the cleavage of $C_\beta–OPh$ and $C_\alpha–OPh$ bonds. Besides the transformation of lignin model compounds, the yield of phenolic monomers from birch wood is up to 32% by using this two-step strategy. The pre-oxidation of $C_\alpha H–$ OH to $C_\alpha=O$ not only weakens the $C_\beta–OPh$ ether bond but also avoids the condensation reactions caused by the presence of C_α^+ from dehydroxylation of $C_\alpha H–$ OH. Furthermore, the NiMo sulfide prefers to catalyze the hydrogenative cleavage of the $C_\beta–OPh$ bond connecting with a $C_\alpha=O$ rather than catalyze the hydrogenation of $C_\alpha=O$ back to original $C_\alpha H–OH$, which further ensures and utilizes the advantages of pre-oxidation.

KEYWORDS:

Lignin, oxidation−hydrogenation, phenolic monomer, $NaNO_2$/DDQ/NHPI, NiMo sulfide, lignin fragments condensation

1
2
3
4
5
6
7
8
9
10
11
12
13
14
15
16
17
18
19
20
21
22
23
24
25
26
27
28
29
30
31
32
33
34
35
36
37
38
39
40
41
42
43
44
45
46
47
48
49
50
51
52
53
54
55
56
57
58
59
60

GRAPHIC ABSTRACT:

1. INTRODUCTION

The increasing awareness of dwindling fossil resources and the ever-increasing need for more aromatic chemical feedstock has led to extensive research into efficient methods to meet this demand. In numerous alternative solutions, lignin has received a great amount of attention, owing to its potential to produce functionalized aromatic fine chemicals.[1] The key issues for the lignin transformation lie in the development of highly selective and active catalysts to effectively cleave the ubiquitous ether bonds, whilst leaving the aromatic benzene rings unconverted.[2] The condensation of generated carbocation intermediates[3] and aldehyde products[4] should also be avoided. It still remains a big challenge for converting lignin models and extracts, albeit original lignin.

In recent years, a lot of works have been directed towards the depolymerization of native lignin residing in wood. Based on the analysis of lignin conversion, products distributions and lignin structure change, containing condensation and rearrangement, this approach termed "lignin-first" has provide much useful guidance in lignin valorization.[5] Besides the "lignin-first" approach, another approach termed "bottom-up" focuses on the mechanism research of the transformation of lignin models and then applies the methods in the lignin conversion. Although a vast difference exists between studies on model compounds and studies on technical/native lignin because of the complex structure of lignin, the "bottom-up" approach has presented many effective catalytic systems and strategies in the technical/native lignin conversion.[6] Nevertheless, each approach has its own advantages and limitations.

Hence, both domains should be complementary in founding efficient methods in lignin conversion.
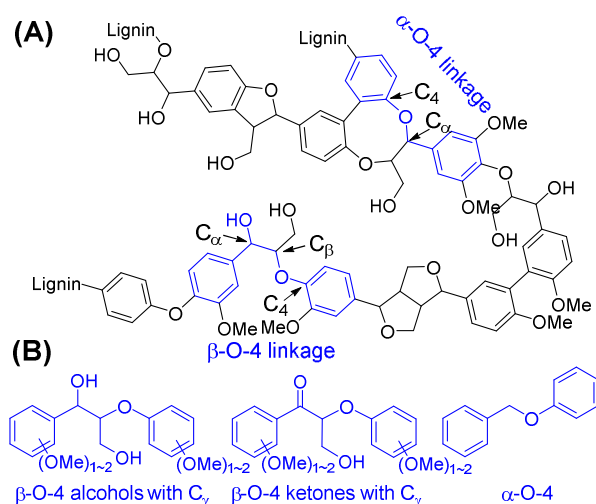

Figure 1. Representative structure of a fragment of lignin (A) and the lignin model compounds (B) used in this study.

The β-O-4 linkage (Figure 1) accounts for 40-60% of interunit linkages in lignin. It is the primary target structure to be broken during lignin depolymerization.[1a] In addition, α-O-4 and 4-O-5 linkages account for about 10% and 5% of interunit linkages. Methods including hydrogenation,[2, 7] transfer hydrogenation,[8] reduction,[9] oxidation,[10] acidolysis,[4, 11] alkaline hydrolysis,[12] alcoholysis[13] and redox-neutral[14] have been used in the transformation of these lignin linkages.

Recently, a two-step strategy has been explored in the transformation of lignin and model compounds. Given the fact that the bond dissociation enthalpy (BDE) of C_β–OPh bond of β-O-4-ketones is about 40~50 kJ·mol^{-1} lower than C_β–OPh bond of β-O-4-alcohols,[15] and the β-O-4-ketones contain active C_β–H and C_α–C_β bonds for further transformation, the C_αH–OH of β-O-4-alcohols is usually pre-converted to

C_α=O by using well-established benzyl alcohol oxidation methods. In the second step of converting β-O-4-ketones, uncatalyzed routes or reduction methods are usually used primarily to avoid the back-conversion to β-O-4-alcohols. Stahl and co-workers[16] found O_2/AcNH-TEMPO/HCl/HNO$_3$ system can realize chemoselective aerobic oxidation of secondary benzylic alcohols within lignin model compounds to ketones. In the subsequent transformation of pre-oxidized β-O-4 linkages, they achieved the selective C_α–C_β bond cleavage with KOH/H_2O_2[16] and C_β–OPh bond cleavage[6a] in presence of formic acid. Stephenson group[17] identified that the photocatalyst [Ir(ppy)$_2$(dtbbpy)]PF$_6$ can achieve the cleavage of C_β−OPh bond within β-O-4-ketones, and the generated fragment can be reduced by HCOOH. Westwood and co-workers[6c] have reported that the DDQ/tBuONO/O_2 system could promote the chemoselective oxidation of C_αH–OH to C_α=O within β-O-4 linkages, and the pre-oxidized β-O-4 linkages could be cleaved by Zn/NH$_4$Cl. Besides the first oxidation or dehydrogenation of C_αH–OH to C_α=O, Barta and co-workers have reported a series of strategies combining acidolysis with etherification, hydrogenation, or decarbonylation reactions.[4a]

We hold the same viewpoint that the two-step methodology is suitable for dissociating interlinking lignin units, but we think the known methods have problems of focusing too much on the first step but understating the following ether conversion. And the reported methods mainly focus on the transformation of β-O-4 linkage. To improve the efficiency of lignin conversion, the transformation of other ether linkages should be also taken into consideration.

Homogeneous catalysts with well-defined structures have been used in catalytic

hydrogenation and transfer hydrogenation cleavage of different C–O–C ether bonds

and C–C bonds. However, in converting original lignin, the homogeneous systems

face all or partial issues as listed in the follows. (1) A contradiction exists between the

specificity of homogeneous systems and the complex structure of lignin. (2) The

competitive coordination to metal active center between ligands and

oxygen-containing groups of lignin. (3) Depolymerizing the stable 3D structure in

solid original lignin into low-molecule-weight fragments for further transformation is

still a challenge for homogeneous systems operated under mild condition. Although

some non-noble heterogeneous catalysts do not have such problems and thus have

drawn much attention in lignin transformation, the harsh reaction conditions make it

difficult to control the reaction selectivity and therefore the obvious transformation of

aromatic rings usually occurs along with the cleavage of target ether bonds.

Another key issue is the possible condensation of lignin fragments at the

existence of acid sites or H^+ species during lignin pretreatment and/or

transformation at high temperature. As shown in Figure 2, three main

condensation processes may happen during the transformation of lignin β-O-4

linkages. (**A**) The aromatic aldehydes generated from the acidolysis of β-O-4

structure with a $C_\alpha H$–OH causes the condensation.[4] (**B**) The C_α^+ of β-O-4

carbocation attacks the adjacent aromatic rings with G or H type and generates

a benzofuran structure after the formation of new C–C bond.[4b, 11a] (**C**) The

generated β-O-4 carbocation intermediate condensates with another G or S type

of aromatic ring.[3] Based on the analysis of these processes, the generation of

β-O-4 carbocation (**1** in Figure 2) is the precondition for the condensation, and

is usually generated from $C_\alpha H$–OH of β-O-4 linkage catalyzed by protonic

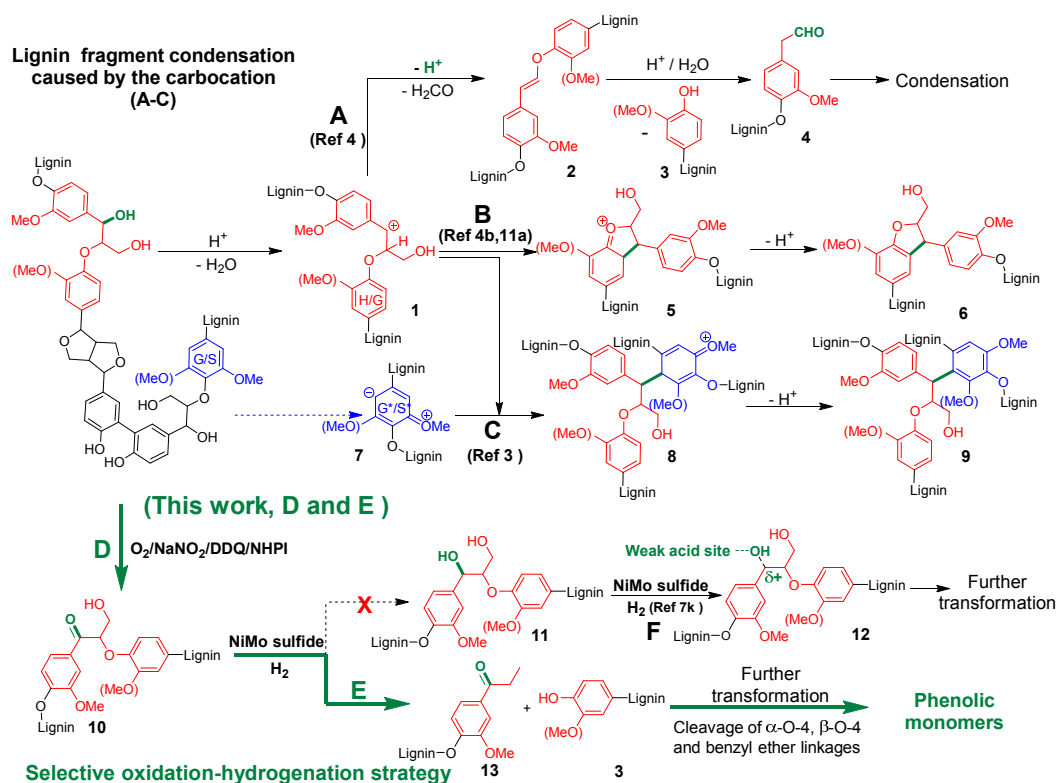acid,[4, 11a] acid sites on the heterogeneous catalysts,[3b] or the acid solvents.[11b, 11c]

Figure 2. The possible condensation processes (A-C) during the transformation of

lignin β-O-4 linkages and our selective oxidation-hydrogenation strategy (D and E).

Condensation caused by the generation of aromatic aldehydes (**A**, Ref 4).

Condensation in the same β-O-4 linkage with a carbocation intermediate **1** (**B**, Ref 4b,

11a). Condensation caused by the condensation of β-O-4 carbocation intermediate **1**

and G/S type of aromatic ring (**C**, Ref 3). Hydrogenolysis of β-O-4 alcohol over the

NiMo sulfide via an $ArCH^{\delta+}CH(CH_2OH)OAr$ intermediate (**F**, Ref 7k). The H, G and

S stand for the *p*-hydroxyphenyl (H)-, guaiacyl (G)- and syringyl (S)-type of lignin

aromatic ring.

To reduce or avoid condensation, guiding the transformation of β-O-4 carbocation or avoiding the generation of β-O-4 carbocation are both crucial. Barta and co-workers[4a] have reported a triflic acid-catalyzed method, which is based on the rapid transformation of in-situ generated substituted phenylacetaldehydes, to achieve the depolymerization of lignin β-O-4 linkages with low condensation products. Luterbacher and co-workers[3a] achieved the goal by etherifying the $C_\alpha H–OH$ and blocking the electron-rich positions at the positions ortho or para to methoxyl in G or S type of aromatic ring with formaldehyde. Furthermore, inspired by the two-step methods containing first conversion of $C_\alpha H–OH$ to $C_\alpha=O$ in β-O-4 model compounds, the combination of selective oxidation and subsequent heterogeneous hydrogenation also should be an effective strategy.[6b] For the advantages of this oxidation-hydrogenation strategy, the first selective transformation of $C_\alpha H–OH$ to $C_\alpha=O$ can not only promote the cleavage of $C_\beta–OPh$ in the hydrogenation process but also prevent the generation of carbocation from $C_\alpha H–OH$.

Although transformation of lignin into aromatic compounds via a two-step strategy, including a first oxidation step to pre-oxidize lignin followed by a subsequent depolymerization is not entirely new, the heterogeneous hydrogenolysis of pre-oxidized lignin structure using H_2 as hydrogen donor still faces some difficulties. An appropriate heterogeneous hydrogenation catalyst should have

the following features. (1) The catalyst prefers to catalyze the cleavage of β-O-4 ether bonds rather than the hydrogenation of aromatic rings and carbonyl groups. (2) The catalyst should have low activity to generate carbocation from substrates containing a $C_{\alpha}H$–OH structure. (3) Besides the β-O-4 linkage, the other ether linkages can be also transformed. (4) For the practical lignin conversion, a non-noble metal catalyst is favorable.

Following the above criteria, we herein used a biomimetic organocatalyst system O_2/NaNO$_2$/DDQ/NHPI to oxidize lignin $C_{\alpha}H$–OH to C_{α}=O within β-O-4 linkages at the first step. In the subsequent hydrogenation of C_{β}–OPh ether bonds, we fortunately found the as-prepared NiMo sulfide catalyst can achieve the selectively hydrogenative cleavage of C_{β}–OPh ether bonds with high yield of aromatic rings. Interestingly, α-O-4 linkage and benzyl ether linkage, which are far less studied in previous works, can also be transformed in the hydrogenation process. Furthermore, we also did some studies towards the identification and rationalization of heterogeneous catalysts for the hydrogenolysis of pre-oxidized lignin model structure.

1
2
3
4
5
6
7
8
9
10
11
12
13
14
15
16
17
18
19
20
21
22
23
24
25
26
27
28
29
30
31
32
33
34
35
36
37
38
39
40
41
42
43
44
45
46
47
48
49
50
51
52
53
54
55
56
57
58
59
60

2. EXPERIMENTAL SECTION

2.1 Materials and lignin model compounds synthesis

All chemicals are of analytical grade and used without further purification. Dibenzyl ether, benzyloxybenzene and diphenyl ether are purchased from Aladdin Chemicals Co., Ltd.

The β-O-4 lignin model compounds including 2-phenoxy-1-phenylethanone (β-O-4-K), other β-O-4-ketones without $C_\gamma H–OH$,[18] 2-phenoxy-1-phenylethanol (β-O-4-A), other β-O-A-alcohols without $C_\gamma H–OH$,[18] (2-phenoxyethyl)benzene (β-O-4-H),[7e] (2-phenoxy-vinyl)benzene (β-O-4-O),[11a] (1-methoxy-2-phenoxyethyl) benzene (β-O-4-E)[8a], 2-methyl-2-phenoxy-1-phenylpropan-1-one (β-O-4-K-2βCH₃),[8e] polymeric β-O-4 lignin model (β-O-4-A-Polymer and β-O-4-K-Polymer),[14e] β-O-4-ketones and β-O-A-alcohols with $C_\gamma H–OH$ structure[13a] are synthesized according to the previous reports. The detailed synthesis procedures of β-O-4 compounds are provided in the Supporting Information.

2.2 Catalysts preparation

The NiMo sulfide catalyst was prepared according to the previously reported procedure.[7k] The $(NH_4)_2MoS_4$ (5.2 g, 20 mmol) was dispersed in a nickel chloride solution (200 mL, 20 mmol). After stirring at 100 °C for 6 h, the solid was collected by filtration, washed with distilled water and ethanol, dried at 60 °C under vacuum, followed by calcination in a horizontal furnace at

450 °C for 6 h in Ar flow (50 mL·min^{-1}) at a 5 °C·min^{-1} heating rate from 25 °C.

The MoS_2 was obtained by treating the as-prepared $(NH_4)_2MoS_4$ in a horizontal furnace at 450 °C for 6 h in an Ar flow. NiS was synthesized according to the previous work.[19] Ni/C (10 w%) was prepared by the impregnation method with $Ni(NO_3)_2$ as the precursor, which was further reduced by hydrogen at 400 °C for 2 h.[7e] The Pd/C (5 wt%) was prepared by a impregnation method with $PdCl_2$ as the precursor, which was pre-reduced at 300 °C in H_2 flow for 3 h before using.

2.3 Characterizations

X-ray diffraction (XRD) characterizations were conducted on a Rigaku D/Max 3400 powder diffraction system with Cu Kα radiation (λ=1.542 Å). The electron microscopy analysis was carried out on the FEI Titan ChemiSTEM at the Ernst Ruska Center Jülich, Germany, equipped with the high solid-angle four quadrant SUPER-X energy dispersive X-ray (EDX) detector and operating at 200 kV.

2.4 The density functional theory calculations

We have performed density functional theory (DFT) calculations using the Vienna ab initio simulation package (VASP),[20] which is a periodic planewave density functional theory implementation. The PAW method,[21] a frozen-core all-electron method using the exact shape of the valence wave functions instead of pseudowave functions, was chosen to describe the electron−ion interactions.

The exchange correlation energy has been calculated within the generalized gradient approximation (GGA) using the PBE functional formulation.[22] An energy cutoff for plane waves of 400 eV was employed throughout this study. To include dispersion interactions, we used the DFT-D3 methodology.[23] For more detailed procedures, please refer to our previous work.[24]

2.5 Procedure for catalytic reactions of model compounds

In a typical selective oxidation experiment, substrate (0.15 mmol), $NaNO_2$ (6 mg), DDQ (8 mg), NHPI (8 mg), CH_3CN (2.5 mL) and a magnetic stirrer were placed into a high-pressured reactor (15 mL). After flushing with O_2, the reactor was charged with 0.5 MPa of O_2 and placed into a preheated red copper mantle at the desired temperature with magnetic stirring.

In a typical hydrogenation experiment, substrate (0.2 mmol), catalyst (20 mg) and methanol (2.0 mL) were placed into a high-pressured reactor (15 mL). After flushing with Ar for five times, the reactor was charged with 1.0 MPa of H_2 and placed into a preheated red copper mantle at the desired temperature with magnetic stirring.

After reaction, the reactor was quenched to ambient temperature using cooling water. The *n*-dodecane as the standard substance in ethanol solution was added in the reaction mixture. After the filtration with a Teflon filter membrane, the organic products are analyzed by GC-FID (Agilent 7890 A) and GC/MS (GC: Agilent 7890 A, MS: Agilent 5975 C).

2.6 Procedure for birch powders transformation

Birch powder was pre-treated with methylbenzene in a Soxhlet extractor for 24 h to remove the soluble substance. The lignin content in birch powders was determined by the TAPPI standard method to be 19 w%.[13a] In the pre-oxidation of birch powder, birch powder 100 mg, acetonitrile 5.0 mL, $NaNO_2$ 8 mg, DDQ 12 mg, NHPI 12 mg and a magnetic stirrer were placed into a high-pressured reactor (15 mL). After flushing with O_2 for five times, the reactor was charged with 1.0 MPa of O_2 and placed into a preheated red copper mantle at 90 °C for 4 h. The pre-oxidative birch powder was collected by filtration, washed with CH_3CN, dried at 60 °C under vacuum. In the hydrogenation process, birch powder or pre-oxidative birch powder 50 mg, methanol 5.0 mL, NiMo sulfide 50 mg and a magnetic stirrer were placed into a high-pressured reactor (15 mL). After flushing with H_2 for five times, the reactor was charged with 1.0 MPa of H_2 and placed into a preheated red copper mantle 200 °C for 4 h. After the reaction, the reactor was quenched to ambient temperature using cooling water. The naphthaline as the standard substance in ethanol solution was added in the reaction mixture, after the filtration with a Teflon filter membrane, the organic products are analyzed by GC-FID (Agilent 7890 A) and GC/MS (GC: Agilent 7890 A, MS: Agilent 5975 C).

3. RESULTS AND DISCUSSION

3.1 The difference between direct hydrogenation and oxidation-hydrogenation of β-O-4 lignin model compounds

The goal of this study is to build an efficient strategy using maneuverable and non-noble hydrogenation catalysts to achieve the selective cleavage of lignin ether bonds. 2-Phenoxy-1-phenylethanol (β-O-4-A), 2-phenoxy-1-phenylethanone (β-O-4-K) and their derivatives with or without C_γH-OH structure were used as β-O-4 linkage model compounds. In addition, benzyloxybenzene represents α-O-4 linkage, and dibenzyl ether represents the normal benzylic ether linkage.

In the direct hydrogenation of β-O-4-A (Chart 1A), Pd/C offered complete conversion (Entry 1), but the selectivity to products with C_β–OPh bond cleavage was only 11%. Most of the products were generated by the hydrogenolysis of C_αH–OH (67%) and hydrogenation of aromatic rings (22%). Our previous work[7e] found that in comparison with Pd/C, Ni/C catalyst with mild hydrogenation activity could not only promote the cleavage of C_β–OPh bond but also increase the yield of aromatic products. But Ni/C catalyst has a drawback that the Ni particles easily get oxidized when being handled in air or during reaction, which will lead to worse conversion of β-O-4-A (Chart 1A, Entry 2).
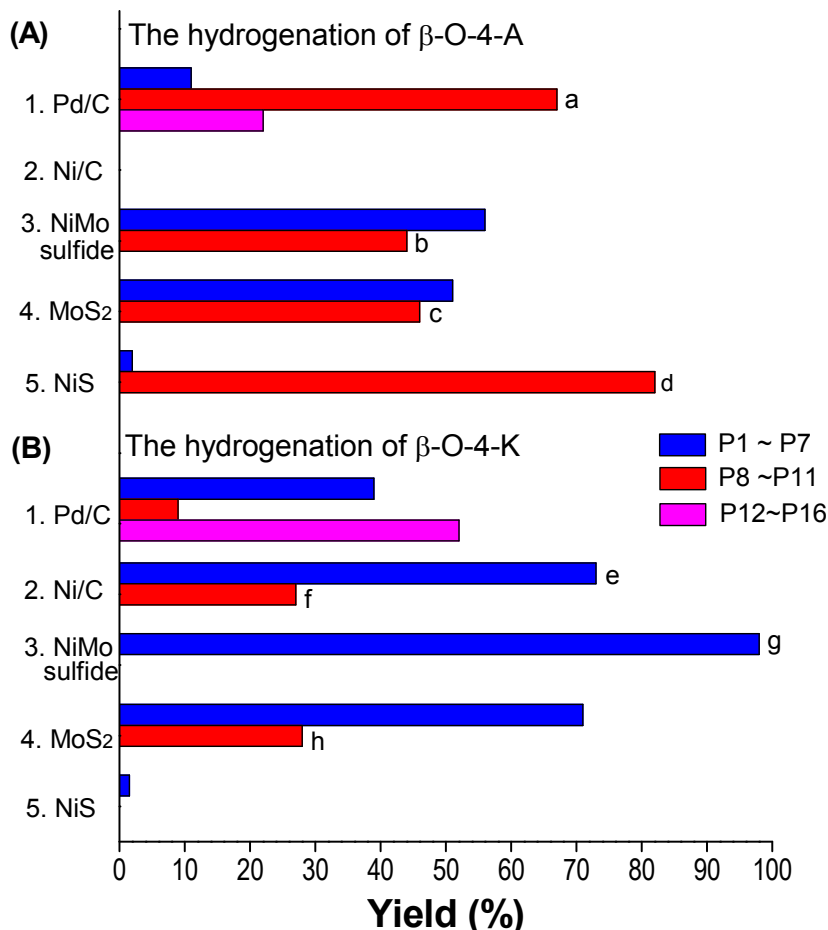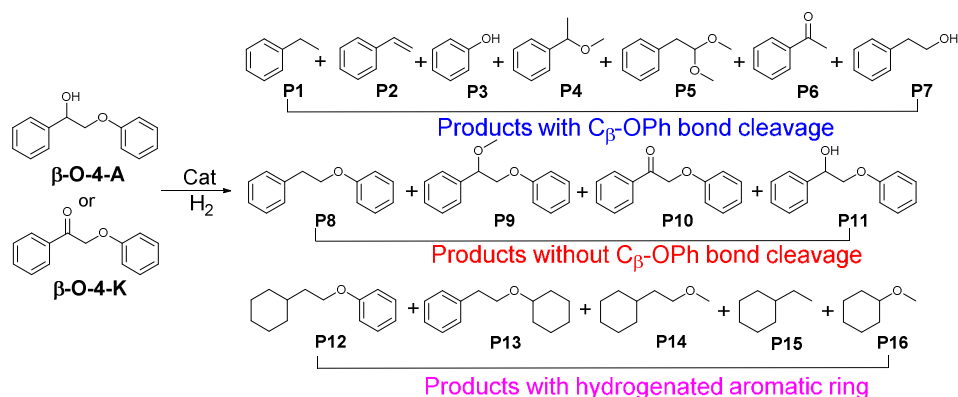
Chart 1. The hydrogenative conversion of β-O-4-A (A) and β-O-4-K (B) over various catalysts. Reaction conditions: substrate 0.2 mmol, catalyst 20 mg, methanol 2.0 mL, 1.0 MPa of H₂, 180 °C, 4 h (β-O-4-A) or 6 h (β-O-4-K). Products distributions: (a) P8 67%; (b) P8 1%, P9 43%; (c) P8 35%, P9 11%; (d)

P9 82%; (e) P3 33%, P6 31%; (f) P11 26%; (g) P3 41%, P6 50%; (h) P8 18%, P9 3%, P11 7%.

In searching for a non-noble metal and stable catalyst, we found Mo-based catalyst with moderate hydrogenation activity was a suitable candidate.[25] Mo-based catalysts preferred to cleave the C–O bond rather than hydrogenate the aromatic rings.[26] Particularly, MoS_2 offered a 97% conversion without aromatic rings being hydrogenated (Chart 1A, Entry 4). But products with C_β–OPh bond cleavage were only 51 %. MoS_2 could also catalyze C_αH–OH hydrogenolysis to $C_\alpha H_2$ (β-O-4-H, 35%) and C_αH–OH etherification to C_αH–OCH_3 (β-O-4-E, 11%). As shown in Scheme S1, the two by-products can restrain the cleavage of C_β–OPh bond. In addition, we modified MoS_2 catalyst with Ni species, and the obtained NiMo sulfide catalyst offered a > 99% conversion of β-O-4-A (Chart 1A, Entry 3) and slightly increased the C_β–OPh cleaved products to 56%. However, the C_αH–OH bond hydrogenolysis to $C_\alpha H_2$ was suppressed (1%), while the C_αH–OH etherification was increased to 43%. To further reduce the etherification products, n-dodecane, 1,4-dioxane, acetonitrile or N-methyl pyrrolidone was used as solvent, but low conversions and high ratio of β-O-4-H were obtained (Scheme S2).

To achieve the selective cleavage of lignin ether bonds, one feasible strategy is to firstly weaken the C_β–OPh bond and then employ a catalytic system targeting on the selective cleavage of target C_β–OPh bond during the subsequent conversion. The pre-oxidization of C_αH–OH to C_α=O can weaken the C_β–OPh bond.[6a, 16-17] So, as discussed in the introduction, the key issue of oxidation-hydrogenation strategy lies in

the selectivity of the subsequent hydrogenation process. The most important feature of catalyst is that the catalyst prefers to catalyze the cleavage of β-O-4 ether bonds rather than achieve the hydrogenation of aromatic rings and generated $C_\alpha=O$ back to $C_\alpha H$–OH.

Then, β-O-4-K with $C_\alpha=O$ was used as the substrate to screen such a hydrogenation catalyst. Except NiS offered a low conversion, Pd/C, Ni/C, MoS_2 and NiMo sulfide all gave > 99% conversions and increase in the yields of products with C_β–OPh bond cleavage, but their product distributions were quite different (Chart 1B). The products with hydrogenated aromatic rings increased to 52% over Pd/C (Chart 1B, Entry 1), and Pd/C could also catalyze the hydrogenation of $C_\alpha=O$ to β-O-4-A and β-O-4-H (9%). Ni/C could catalyze the hydrogenation of β-O-4-K to β-O-4-A (26%). When the hydrogenation of β-O-4-K was catalyzed by MoS_2, the main products were target aromatic products with C_β–OPh bond cleavage (71%), but a part of β-O-4-K was still transformed to β-O-4-A (7%), β-O-4-H (18%) and β-O-4-E (3%). We then found that the NiMo sulfide catalyst was an appropriate catalyst for the hydrogenative cleavage of C_β–OPh bond within β-O-4-K. The main products were acetophenone and phenol generated from C_β–OPh bond cleavage. This confirmed the feasibility of selective oxidation-hydrogenation strategy in the degradation of lignin and its model compounds. We then focused on the establishment of catalytic system and research about hydrogenation mechanism and factors on the reaction selectivity (vide infra).

3.2 Selective oxidation of lignin model compounds over the NaNO₂/DDQ/NHPI organocatalyst system

For the selective oxidation of targeted benzyl alcohols, referring to our previous works about organocatalyst systems containing the combination of various quinones and N-hydroxyphthalimide (NHPI),[27] we found that $NaNO_2$/DDQ/NHPI organocatalyst system could efficiently catalyze the selective oxidation of β-O-4-A to β-O-4-K with O_2. A 99% conversion and 95% selectivity to β-O-4-K was obtained in 2 h at 80 °C (Table 1, Entry 1). In the selective oxidation of β-O-4-A, each composition of the $NaNO_2$/DDQ/NHPI organocatalyst system was necessary (Table S1, Entry 1-7). When $^{18}O_2$ was used as the oxidant, no ^{18}O labelled β-O-4-K was checked (Table S1, Entry 9), which indicated an oxidative dehydrogenation process.
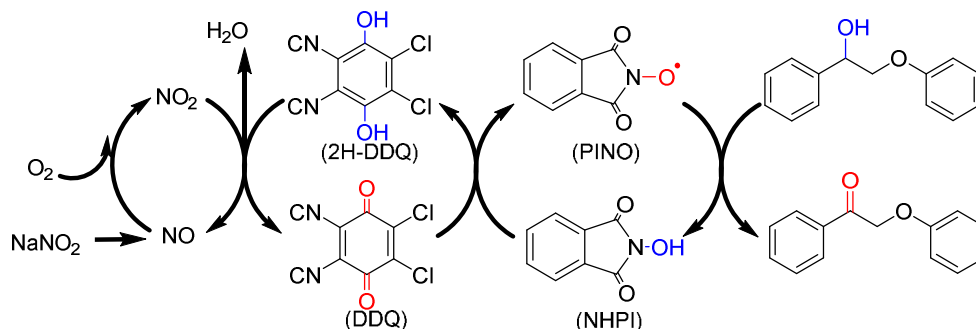
Scheme 1. Proposed catalytic cycle for the oxidation of β-O-4-A to β-O-4-K

As reported in previous researches, the NO_x generated from the $NaNO_2$ decomposition can catalyze the hydroquinone oxidation to quinone with O_2,[27b] and the quinone can abstract H atom from NHPI and promote the generation of PINO (phthalimide-N-oxyl) radical, which is confirmed by the UV-Vis spectroscopy.[27c] Herein, we propose the mechanism of the β-O-4-A oxidation (Scheme 1): (1) DDQ abstracts a hydrogen atom from NHPI to generate a highly reactive PINO free radical and hydroquinone (2H-DDQ); (2) PINO radicals obtain hydrogen atoms from

β-O-4-A to generate NHPI and β-O-4-K; (3) NO molecules generated from NaNO$_2$

decomposition in the reaction media catalyze the oxidation of hydroquinone

(2H-DDQ) to quinone (DDQ) with O$_2$.[27d]

The O$_2$/NaNO$_2$/DDQ/NHPI catalytic system also showed excellent selectivity

and reactivity in the oxidation of the other benzyl alcohols (Table 1, 1b-g). The

expected β-O-4-ketones were obtained in good yields (2b-g). The catalytic system

also showed excellent selectivity toward the oxidation of benzylic alcohol than the

hydroxymethyl group at C$_\gamma$ (2e, 2g). While the intermediate or β-O-4-ketone product

could lose a H$_2$O to generate a C$_\beta$=C$_\gamma$ bond during the oxidation process (2e-2, 2g-2).

The O$_2$/NaNO$_2$/DDQ/NHPI catalytic system shows low activity in the selective

oxidation of α-O-4 model compound.

Table 1. The selective oxidation of C$_\alpha$–OH in lignin model compounds [a]
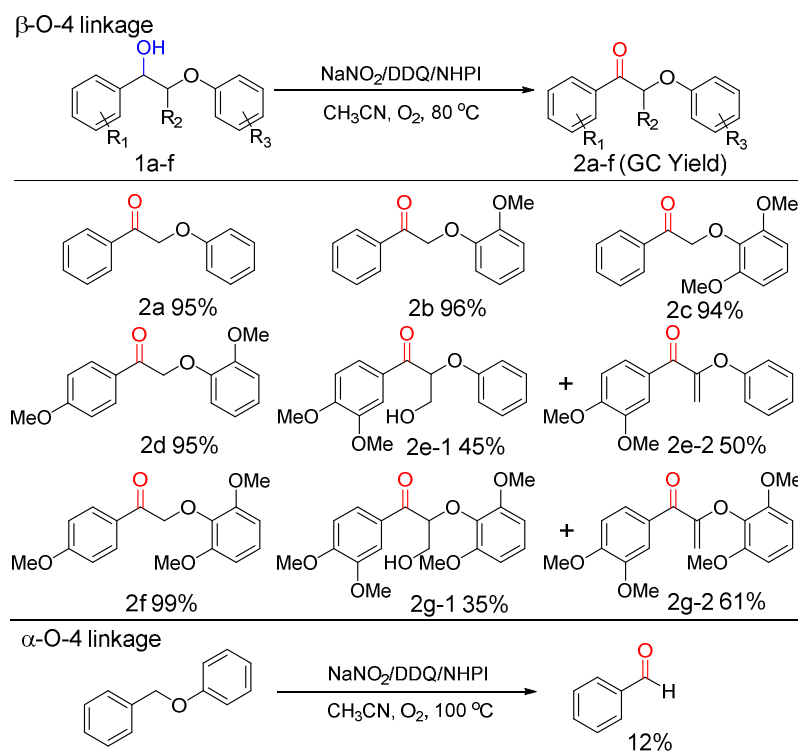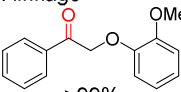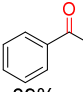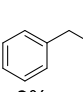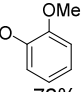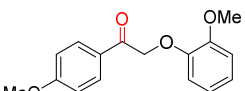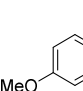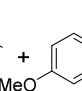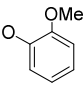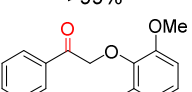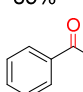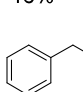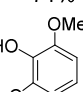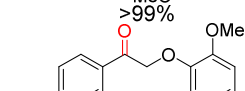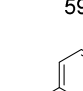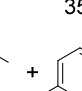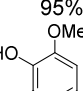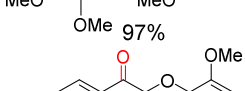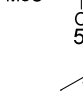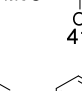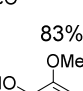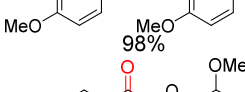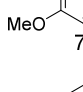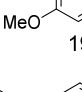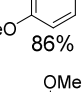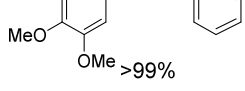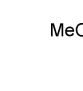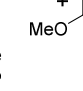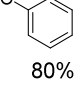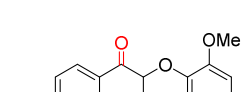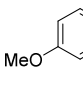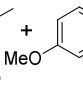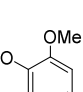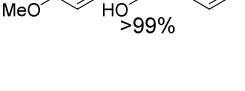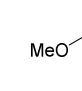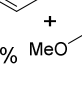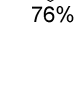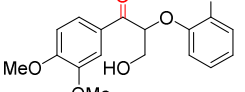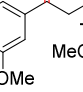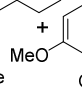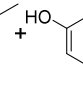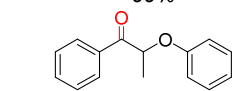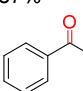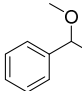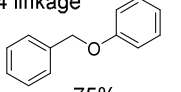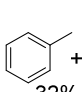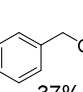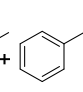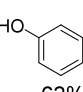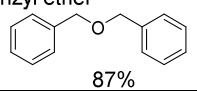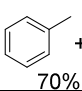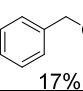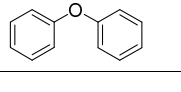
[a] Reaction conditions: substrate 0.15 mmol, NaNO$_2$ 6 mg, DDQ 8 mg, NHPI 8 mg, CH$_3$CN 2.5 mL, O$_2$ 0.5 MPa, 80 °C, 2 h.

3.3 Selectively hydrogenative cleavage of ether bonds in lignin model compounds over the NiMo sulfide

Then, we checked the selective hydrogenation of β-O-4-ketones and other ether linkages over the NiMo sulfide catalyst. As shown in Table 2, > 97% conversions were obtained in the hydrogenation of different β-O-4-ketones, and no products with hydrogenated aromatic ring was detected. NiMo sulfide selectively catalyzed the hydrogenative cleavage of C$_\beta$–OPh bond. And the ether bond of methoxyl group connected with aromatic ring is unchanged. Given the fact that the β-O-4 compound with a C$_\alpha$H$_2$ is difficult to be transformed over the NiMo sulfide (Scheme S1), the products of ethylbenzene and its analogues should generate from the hydrogenation of products like acetophenone or the fragments of β-O-4-ketones. Furthermore, the NiMo sulfide could also catalyze the hydrogenative cleavage of ether bonds of dibenzyl ether and α-O-4 model compound (benzyloxybenzene). No product was generated in the hydrogenation of diphenyl ether.

1
2
3
4
5
6
7
8
9
10
11
12
13
14
15
16
17
18
19
20
21
22
23
24
25
26
27
28
29
30
31
32
33
34
35
36
37
38
39
40
41
42
43
44
45
46
47
48
49
50
51
52
53
54
55
56
57
58
59
60

Table 2. The selective hydrogenation of lignin model compounds [a]

Substrate (Conversion)	Products (GC yield)

β-O-4 linkage

α-O-4 linkage

Benzyl ether

4-O-5 linkage

no reaction

[a] Reaction conditions: substrate 0.2 mmol, NiMo sulfide 20 mg, methanol 2.0 mL, H_2 1.0 MPa, 180 °C, 6 h.

Although the pre-oxidation of $C_\alpha H–OH$ to $C_\alpha=O$ can weaken the $C_\beta–OPh$ bond and prevent the generation of β-O-4 carbocation from dehydroxylation at C_α, given the possibility that the $C_\alpha=O$ group of β-O-4-ketones can be hydrogenated to $C_\alpha H–OH$ in the following hydrogenation (Figure 2, **D** and **E**), the condensation problem may arise again. However, the as-synthesized NiMo sulfide prefers to catalyze the cleavage of $C_\beta–OPh$ rather than hydrogenate the $C_\alpha=O$ group of β-O-4-ketones (Table 2). Furthermore, as shown in our previous work,[7k] the weak and medium strong acid sites (Figure S12) of NiMo sulfide cannot promote the generation of β-O-4 carbocation with the active C_α^+ structure for the condensation processes. As experimental evidences, the acid sites of heterogeneous NiMo sulfide cannot efficiently catalyze the acidolysis of β-O-4-A and β-O-4-O under Ar atmosphere (Scheme S3). However, the NiMo sulfide can catalyze the further transformation of β-O-4-A via an absorbed $ArCH^{\delta+}CH_2OAr$ intermediate under H_2 atmosphere (Figure 2, **F**).[7k] But the part of etherification products at C_α without cleavage of $C_\beta–OPh$ bond (Chart 1A, Entry 3) restricts the direct hydrogenation of β-O-4-alcohols over the NiMo sulfide. So, the two-step oxidation-hydrogenation is an efficient strategy, and the NiMo sulfide is an appropriate non-noble metal hydrogenation catalyst to realize this strategy.

3.4 Mechanism of β-O-4-K conversion over the NiMo sulfide

Next, we propose our understanding about the high selectivity of the hydrogenation process over NiMo sulfide.
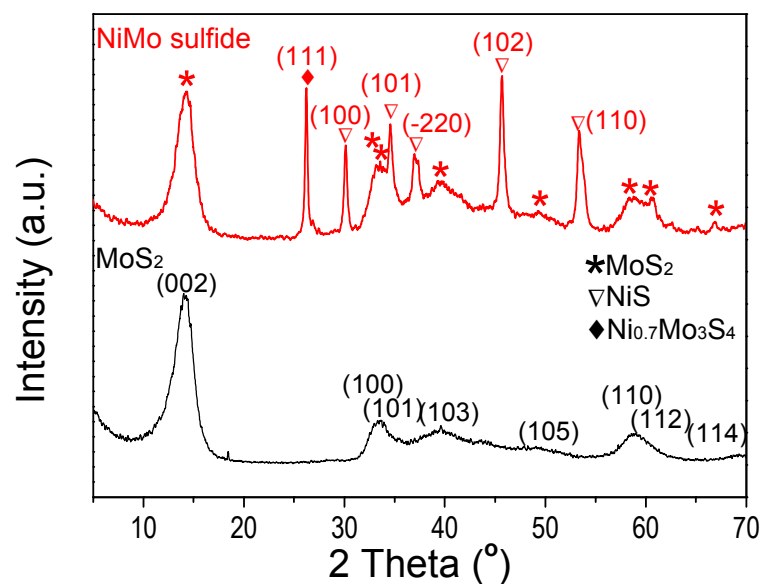
Figure 3. XRD patterns of the NiMo sulfide and MoS_2 catalysts.

As shown in Figure 3, MoS_2 and NiS phase peaks exist in the XRD pattern of the NiMo sulfide catalyst. Besides these peaks, there are also peaks attributed to $Ni_{0.7}Mo_3S_4$, which is one of the Ni doped heterometallic cubane-type Mo clusters. Element mapping by EDX (Figure S13c-f) show that the Mo and S species are uniformly distributed, and the Ni species appears aggregated to about 10 nm in some zones, which corresponds to the fact that a NiS phase and $Ni_{0.7}Mo_3S_4$ phase exist in the XRD pattern of the NiMo sulfide catalyst.
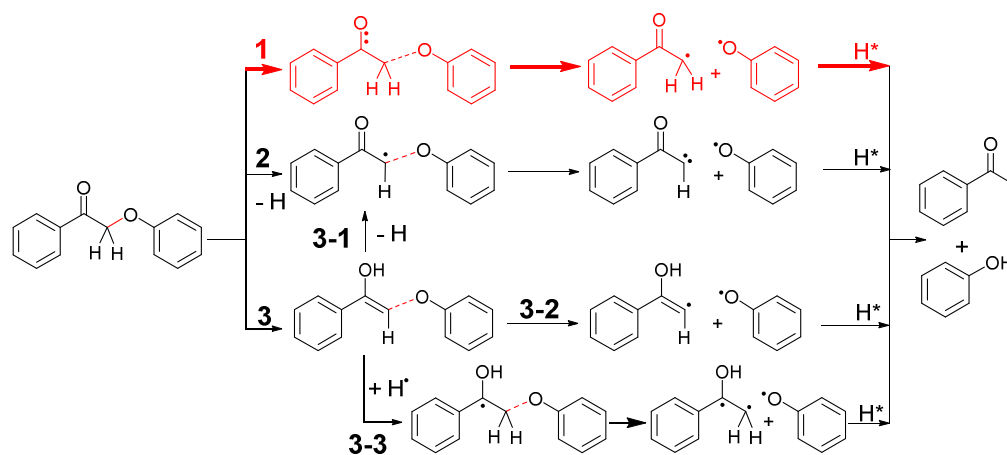
Scheme 2. The routes for the β-O-4-K conversion over the NiMo sulfide catalyst

Given the intricate structure of heterogeneous NiMo sulfide catalyst (Figure 3) and complex degradation process of simple β-O-4-K,[8a, 8d, 8e, 14d, 14e, 18, 24, 28] it is an efficient method to describe the structure-activity relationship and factors on the system selectivity by analyzing the transformation of the substrate.[7k] Regarding acetophenone and phenol as the target products, herein, we propose the potential routes of β-O-4-K transformation with detailed process of bonds cleavage (Scheme 2). (**Route 1**) β-O-4-K adsorbs on the heterogeneous catalyst and transforms to activated β-O-4-K with an activated C_α=O group, then cleavage of C_β–OPh ether bond occurs and the generated intermediates (PhCOCH$_2$· and PhO·) are hydrogenated to PhCOCH$_3$ and PhOH.[8a, 8d] (**Route 2**) β-O-4-K loses an H$_\beta$ and transforms to adsorbing intermediates (PhCOCH·· and PhO·) after the cleavage of C_β–OPh bond, which are subsequently hydrogenated to PhCOCH$_3$ and PhOH.[8e, 14e, 24] (**Route 3-1**) The generation of adsorbing PhCOCH·OPh intermediate is promoted by a keto-enol tautomerism of β-O-4-K to PhC(OH)=CHOPh,[24] then PhCOCH·OPh intermediate transforms to PhCOCH$_3$ and PhOH. (**Route 3-2**) The enol intermediate can also

transform to adsorbing PhC(OH)=CH$^{\bullet}$ and PhO$^{\bullet}$ species via the cleavage of C–OPh bond, which are hydrogenated to PhCOCH$_3$ and PhOH. (**Route 3-3**) The absorbing enol intermediate (PhC(OH)=CHOPh) reacts with a H$^{\bullet}$ species, and the generated adsorbing PhC$^{\bullet}$(OH)CH$_2$OPh transforms to PhC(OH)=CH$_2$ and PhO$^{\bullet}$ via a dearyloxylation process.[7k, 14a, 14c] The PhC(OH)=CH$_2$ transforms to PhCOCH$_3$ via a keto-enol tautomerism, and PhO$^{\bullet}$ is hydrogenated to PhOH.

To check the cleavage order of the corresponding bonds in β-O-4-K, the deuterium labelling experiment and shielding experiment with methyl substituent were carried out.[8e] Given the catalysis of MoS$_2$ based catalysts in H/D exchange reaction,[29] the H or D atoms connecting with C$_\beta$ atom within β-O-4-K and acetophenone could exchange with the solvent H species. Detecting the reaction route by kinetic isotope effect[8e] and amount of D atoms in the product acetophenone[13a] were not entirely accurate methods in this catalytic system (Scheme S5). Furthermore, based on the comparison of these routes, the pre-activation of C$_\beta$–H bond was a key step for the conversion of β-O-4-K in Route 2 and Route 3, while the Route 1 involved the direct hydrogenative cleavage the C$_\beta$–OPh bond. We then used β-O-4-K-2βCH$_3$ as the substrate to check the effect of C$_\beta$–H activation on the cleavage of C$_\beta$–OPh bond (Scheme 3). The NiMo sulfide could catalyze the selective cleavage of β-O-4-K-2βCH$_3$ to 2-methyl-1-phenylpropan-1-one and PhOH, and the conversion of C$_\beta$–OPh bond reached to 98%. This result indicated that Route 1 with direct cleavage of C$_\beta$–OPh bond was possibly the main route of β-O-4-K transformation over the NiMo sulfide.

β-O-4-K-2βCH₃
Conv. 98%

Products GC yield:
88%   6%   3%   83%
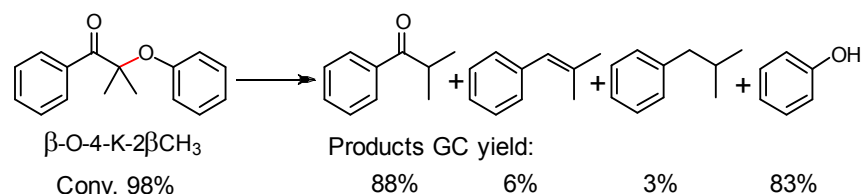
Scheme 3. The cleavage of C$_\beta$–OPh bond in β-O-4-K-2βCH$_3$ over the NiMo sulfide catalyst. Reaction condition: substrate 0.2 mmol, NiMo sulfide 20 mg, methanol 2.0 mL, H$_2$ 1.0 MPa, 180 °C, 6 h.

The reaction route of β-O-4-K transformation over the NiMo sulfide via Route 1 is different from the process over the Pd surface via Route 3-1,[14e, 24, 28a] but it is similar to the homogeneous Ru[8d] or V[14a] catalysts with single active site. We then checked the DFT adsorption models of β-O-4-K over different heterogeneous catalysts. As shown in Figure 4A and 4B, two aromatic rings of β-O-4-K tend to adsorb on the Pd(111) surface and Ni(111) surface with a "face-face" model. The active Pd site has the ability and opportunity to active the C$_\beta$–H bond to transform β-O-4-K to PhCOCH˙OPh for the following transformation with a low activation energy.[14e, 24] At the same time, based on the adsorption model of β-O-4-K over Pd(111) surface and Ni(111) surface, the metal sites around the β-O-4-K can also catalyze the hydrogenation of aromatic rings and carbonyl group (Chart 1B, Entries 1 and 2). When MoS$_2$ with 2D layer structure is used as catalyst, the β-O-4-K tends to adsorb at the edge Mo sites of MoS$_2$. Given that hydrogenative Mo sites are in a linear arrangement (Figure 4C), besides the Mo sites working as active site to cleave C$_\beta$–OPh bond, there are few Mo sites work as the side reaction centers for the hydrogenation of aromatic rings, which lead to the high yield of aromatic rings over the MoS$_2$. However, the Mo sites around the C$_\alpha$=O group of adsorbed β-O-4-K can

also work as active sites for the hydrogenation of C_α=O, which leads to the high yield

of β-O-4-H (Chart 1B, Entry 4).
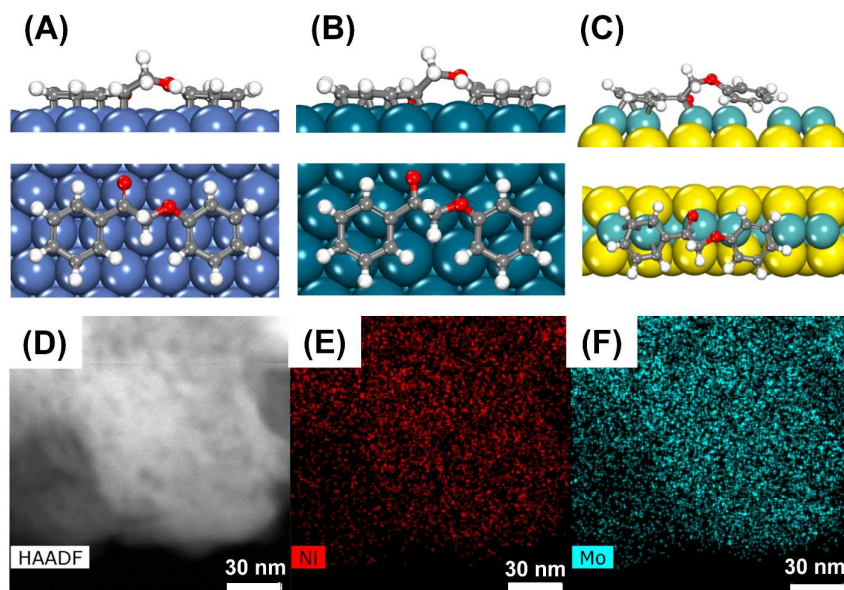
Figure 4. The DFT adsorption models of β-O-4-K on Ni(111), Pd(111) and MoS$_2$ (Mo

edge) (A-C), annular dark-field scanning transmission electron microscopy image of

NiMo sulfide (D). (E, F) show the element maps of Ni and Mo from energy dispersive

X-ray analysis.

Compared with the catalytic performance of MoS$_2$, introducing NiS$_x$ species in

the NiMo sulfide catalyst can obviously increase the selectivity to the hydrogenative

cleavage of C_β–OPh bond rather than the hydrogenation of C_α=O. As shown in Figure

3, MoS$_2$, NiS and Ni$_{0.7}$Mo$_3$S$_4$ phases exist in the NiMo sulfide. When NiS is used as

catalyst, the β-O-4-K conversion is only 1.5% (Chart 1B, Entry 5). The low activity

indicates that the NiS$_x$ species might just be the catalytic promoter to the NiMo

sulfide catalyst. Given that Ni$_{0.7}$Mo$_3$S$_4$ has the similar cubane-type Mo clusters

structure with MoS_2, if its edge Mo atoms are partly replaced by the low active Ni^{2+},

the potential side reaction sites of the hydrogenation of C_α=O can be reduced, and the

yield of aromatic products generated from the cleavage of C_β–OPh bond can increase

(Chart 1B, Entry 3). As shown in Figure 4D-F, the EDX images show that Ni and Mo

atoms are equally distributed at some zones of NiMo sulfide. So, we propose that the

hydrogenative Mo sites in NiMo sulfide are not in a good linear arrangement like

MoS_2 but interrupted by the Ni^{2+}.

To sum up, because of the characteristic of hydrogenative Mo sites in NiMo

sulfide, the adsorption model of β-O-4-K and modest hydrogenative ability of NiMo

sulfide adjusted by the NiS_x species, the NiMo sulfide prefers to promote the

hydrogenative cleavage of C_β–OPh bond rather than catalyze the hydrogenation of

C_α=O in the activated β-O-4-K.

3.5 The depolymerization of polymeric β-O-4 lignin model and birch powders

For the heterogeneous hydrogenation of lignin, the reaction between solid catalyst

and solid substrate remains a challenge.[13a] In this work, besides the model compounds

of ether monomer, we also checked the application of the selective

oxidation-hydrogenation strategy in the conversion of polymeric β-O-4 lignin model

(Scheme 4). In the first oxidation of β-O-4-A-polymer, no obvious monomer products

were detected in the liquid phase (Figure S14). The solid product was easily filtered

and washed with acetonitrile, and its FT-IR spectrum indicated the selective oxidation

of C_α–OH to C_α=O (Figure S15). Further hydrogenation over the NiMo sulfide

catalyst offered a 92% yield of phenolic monomers in 8 h (Scheme 4).
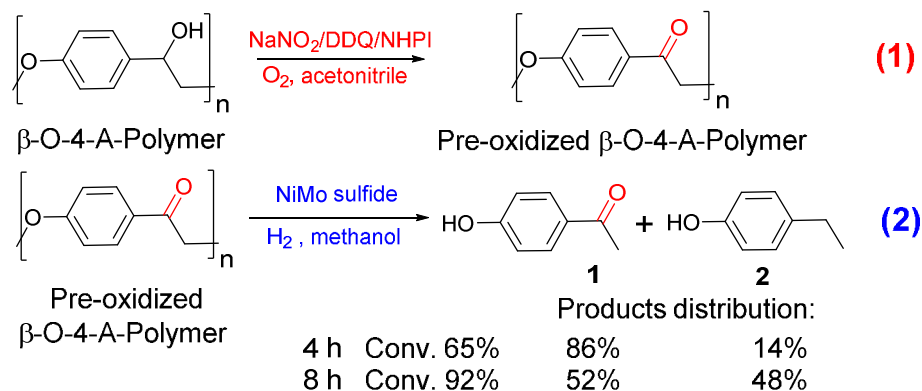
Scheme 4. Transformation of polymeric β-O-4 model. Reaction conditions: (1) β-O-A-Polymer 50 mg, NaNO$_2$ 9 mg, DDQ 12 mg, NHPI 12 mg, O$_2$ 1.0 MPa, acetonitrile 2.5 mL, 80 °C, 3 h; (2) Pre-oxidized β-O-A-Polymer 25 mg, NiMo sulfide 20 mg, methanol 2.5 mL, H$_2$ 1.0 MPa, 180 °C.

These results provided the basis for testing the reactivity of original lignin polymer. Birch is a representative hardwood, which contains about 20 wt% lignin.[13a] As shown in Scheme 5A, the direct hydrogenation of birch powders over the NiMo sulfide only gave a 3% yield of phenolic monomers. After the first treatment under the selective oxidation conditions, the pre-oxidized birch powders were transformed to phenolic monomers with a 32% yield (Scheme 5B). Based on the analysis of the monomer products (Figure S16), the NiMo sulfide catalyst is an appropriate catalyst to keep the aromatic benzene rings unconverted under the relative mild hydrogenative condition.
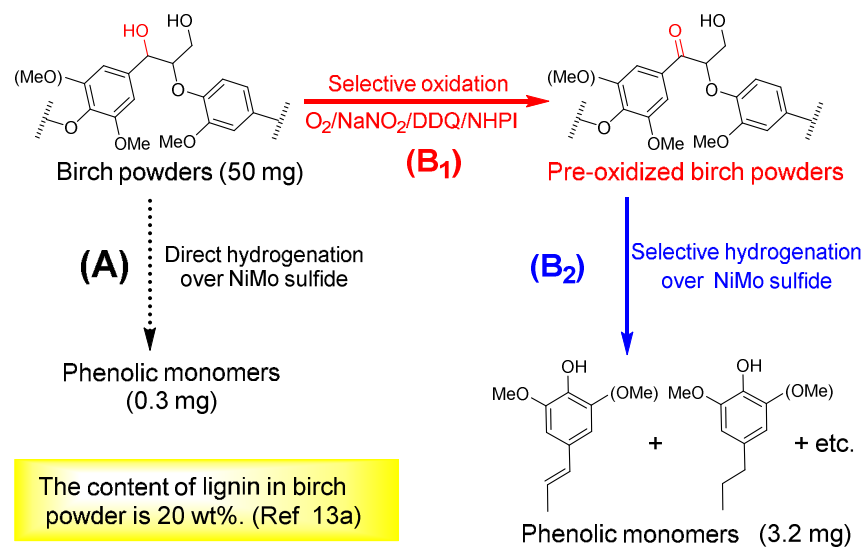
Scheme 5. The conversion of birch powder to aromatic phenolic monomers with direct hydrogenation strategy (A) and oxidation-hydrogenation strategy (B1 + B2). The detailed procedures for each process are provided in the experimental section.

To efficiently catalyze the depolymerization of the lignin in birch powder, we carried out the reaction in methanol at 200 °C,[13a] which could enhance the hydrogenation of the ketone monomers. And the generated alcohol monomers could be further hydrogenated to propyl- substituted compounds or lost a water to propenyl- substituted compounds (Table 2, Entries 7-9). In the hydrogenation of the pre-oxidized birch lignin, the yield of propenyl- substituted compound is higher than the propyl- substituted compound, which is different from the direct hydrogenation of isolated birch lignin (Figure S18) and other hydrogenation process.[13a, 30] We here propose a fragmentation–hydrogenolysis process[13a] (Figure S22) for the second

hydrogenation, which could explain why the main products were not the ketones monomers.

As discussed above, the pre-oxidation treatment to weaken the ether bonds and selective hydrogenation characteristic of NiMo sulfide catalyst could be the main reasons for the high yield of phenolic monomers. Furthermore, the relatively mild and controllable hydrogenative process can reduce the possibility of condensation caused by the carbocation. However, given the facts that NiMo sulfide is not an effective catalyst to cleave the 4-O-5 linkage (Table 2, entry 12) and the lignin conversion needs to be improved, further work aiming at the improvement of activity of catalysts basing on this oxidation-hydrogenation strategy are necessary.

4. CONCLUSIONS

In order to efficiently transform lignin to aromatics, we herein present an oxidation-hydrogenation strategy to selectively cleave the stable and ubiquitous ether bonds. The selective oxidation of $C_\alpha H$–OH to C_α=O in β-O-4 model compounds is firstly achieved by an O_2/NaNO$_2$/DDQ/NHPI system, which not only weakens the target C_β–OPh bond for the further hydrogenolysis but also eliminates the possibility of β-O-4 carbocation generation from $C_\alpha H$–OH to restrain the condensation of lignin fragments. In the second step, the α-O-4 structure and pre-oxidized β-O-4 structure with C_α=O are further hydrogenated over a NiMo sulfide catalyst, leading to the cleavage of C_β–OPh and C_α–OPh bonds to aromatics. As another crucial point for the success of this oxidation-hydrogenation strategy, the NiMo sulfide catalyst prefers to catalyze the direct hydrogenative cleavage of the C_β–OPh bond connecting with a

C_α=O structure rather than catalyze the hydrogenation of C_α=O to C_αH–OH. Furthermore, a 32% yield of phenol monomers from birch powder is obtained by adopting this two-step strategy.

ASSOCIATED CONTENT

Ⓢ Supporting Information

The Supporting Information is available free of charge on the ACS Publications website at DOI:xxxx

β-O-4 lignin model compounds synthesis, catalysts preparation and characterizations, control experiments.

AUTHOR INFORMATION

Corresponding Author

*E-mail for Feng Wang: wangfeng@dicp.ac.cn

Note

The authors declare no competing financial interest.

ACKNOWLEDGMENTS

REFERENCES

(1) (a) Zakzeski, J.; Bruijnincx, P. C. A.; Jongerius, A. L.; Weckhuysen, B. M. *Chem. Rev.* **2010**, *110*, 3552-3599; (b) Zakzeski, J.; Jongerius, A. L.; Bruijnincx, P. C. A.; Weckhuysen, B. M. *ChemSusChem* **2012**, *5*, 1602-1609; (c) Li, C.; Zhao, X.; Wang, A.; Huber, G. W.; Zhang, T. *Chem. Rev.* **2015**, *115*, 11559-11624; (d) Rinaldi, R.; Jastrzebski, R.; Clough, M. T.; Ralph, J.; Kennema, M.; Bruijnincx, P. C. A.; Weckhuysen, B. M. *Angew. Chem. Int. Ed.* **2016**, *55*, 8164-8215; (e) Galkin, M. V.; Samec, J. S. M. *ChemSusChem* **2016**, *9*, 1544-1558.

(2) (a) Sergeev, A. G.; Hartwig, J. F. *Science* **2011**, *332*, 439-443; (b) Sergeev, A. G.; Webb, J. D.; Hartwig, J. F. *J. Am. Chem. Soc.* **2012**, *134*, 20226-20229.

(3) (a) Li, S.; Amiri, M. T.; Questell-Santiago, Y. M.; Héroguel, F.; Li, Y.; Kim, H.; Meilan, R.; Chapple, C.; Ralph, J.; Luterbacher, J. S. *Science* **2016**, *354*, 329-333; (b) Bouxin, F. P.; McVeigh, A.; Tran, F.; Westwood, N. J.; Jarvis, M. C.; Jackson, S. D. *Green Chem.* **2015**, *17*, 1235-1242.

(4) (a) Deuss, P. J.; Scott, M.; Tran, F.; Westwood, N. J.; de Vries, J. G.; Barta, K. *J. Am. Chem. Soc.* **2015**, *137*, 7456-7467; (b) Lahive, C. W.; Deuss, P. J.; Lancefield, C. S.; Sun, Z. H.; Cordes, D. B.; Young, C. M.; Tran, F.; Slawin, A. M. Z.; de Vries, J. G.; Kamer, P. C. J.; Westwood, N. J.; Barta, K. *J. Am. Chem. Soc.* **2016**, *138*, 8900-8911.

(5) (a) De, S.; Zhang, J.; Luque, R.; Yan, N. *Energy Environ. Sci.* **2016**, *9*, 3314-3347; (b) Ferrini, P.; Rezende, C. A.; Rinaldi, R. *ChemSusChem* **2016**, *9*, 3171-3180; (c) Ferrini, P.; Rinaldi, R. *Angewandte Chemie International Edition* **2014**, *53*, 8634-8639; (d) Galkin, M. V.; Samec, J. S. M. *ChemSusChem* **2014**, *7*, 2154-2158; (e) Renders, T.; Van den Bosch, S.; Vangeel, T.; Ennaert, T.; Koelewijn, S.-F.; Van den Bossche, G.; Courtin, C. M.; Schutyser, W.; Sels, B. F. *ACS Sustainable Chem. Eng.* **2016**, *4*, 6894-6904; (f) Yan, N.; Zhao, C.; Dyson, P. J.; Wang, C.; Liu, L. T.; Kou, Y. *ChemSusChem* **2008**, *1*, 626-629.

(6) (a) Rahimi, A.; Ulbrich, A.; Coon, J. J.; Stahl, S. S. *Nature* **2014**, *515*, 249-252; (b) Bruijnincx, P. C. A.; Weckhuysen, B. M. *Nat. Chem.* **2014**, *6*, 1035-1036; (c) Lancefield, C. S.; Ojo, O. S.; Tran, F.; Westwood, N. J. *Angew. Chem. Int. Ed.* **2015**, *54*, 258-262.

(7) (a) He, J.; Zhao, C.; Lercher, J. A. *J. Am. Chem. Soc.* **2012**, *134*, 20768-20775; (b) Song, Q.; Wang, F.; Xu, J. *Chem. Commun.* **2012**, *48*, 7019-7021; (c) Wang, X. Y.; Rinaldi, R. *ChemSusChem* **2012**, *5*, 1455-1466; (d) Zhao, C.; Lercher, J. A. *ChemCatchem* **2012**, *4*, 64-68; (e) Song, Q.; Cai, J.; Zhang, J.; Yu, W.; Wang, F.; Xu, J. *Chin. J. Catal.* **2013**, *34*, 651-658; (f) Parsell, T. H.; Owen, B. C.; Klein, I.; Jarrell, T. M.; Marcum, C. L.; Haupert, L. J.; Amundson, L. M.; Kenttamaa, H. I.; Ribeiro, F.; Miller, J. T.; Abu-Omar, M. M. *Chem. Sci.* **2013**, *4*, 806-813; (g) Zhang, J.; Teo, J.; Chen, X.; Asakura, H.; Tanaka, T.; Teramura, K.; Yan, N. *ACS Catal.* **2014**, *4*, 1574-1583; (h) Zhang, J.; Asakura, H.; van Rijn, J.; Yang, J.; Duchesne, P.; Zhang, B.; Chen, X.; Zhang, P.; Saeys, M.; Yan, N. *Green Chem.* **2014**, *16*, 2432-2437; (i) Barta, K.; Warner, G. R.; Beach, E. S.; Anastas, P. T. *Green Chem.* **2014**, *16*, 191-196; (j) Konnerth, H.; Zhang, J.; Ma, D.; Prechtl, M. H. G.; Yan, N. *Chem. Eng.*

Sci. **2015**, *123*, 155-163; (k) Zhang, C.; Lu, J.; Zhang, X.; MacArthur, K.; Heggen, M.; Li, H.; Wang, F. *Green Chem.* **2016**, *18*, 6545-6555

(8) (a) Nichols, J. M.; Bishop, L. M.; Bergman, R. G.; Ellman, J. A. *J. Am. Chem. Soc.* **2010**, *132*, 12554-12555; (b) Barta, K.; Matson, T. D.; Fettig, M. L.; Scott, S. L.; Iretskii, A. V.; Ford, P. C. *Green Chem.* **2010**, *12*, 1640-1647; (c) Li, C. Z.; Zheng, M. Y.; Wang, A. Q.; Zhang, T. *Energy Environ. Sci.* **2012**, *5*, 6383-6390; (d) Chmely, S. C.; Kim, S.; Ciesielski, P. N.; Jimenez-Oses, G.; Paton, R. S.; Beckham, G. T. *ACS Catal.* **2013**, *3*, 963-974; (e) Galkin, M. V.; Sawadjoon, S.; Rohde, V.; Dawange, M.; Samec, J. S. M. *ChemCatchem* **2014**, *6*, 179-184; (f) vom Stein, T.; den Hartog, T.; Buendia, J.; Stoychev, S.; Mottweiler, J.; Bolm, C.; Klankermayer, J.; Leitner, W. *Angew. Chem. Int. Ed.* **2015**, *54*, 5859-5863.

(9) Ren, Y. L.; Yan, M. J.; Wang, J. J.; Zhang, Z. C.; Yao, K. S. *Angew. Chem. Int. Ed.* **2013**, *52*, 12674-12678.

(10) (a) Zakzeski, J.; Jongerius, A. L.; Weckhuysen, B. M. *Green Chem.* **2010**, *12*, 1225-1236; (b) Zakzeski, J.; Bruijnincx, P. C. A.; Weckhuysen, B. M. *Green Chem.* **2011**, *13*, 671-680; (c) Hanson, S. K.; Wu, R. L.; Silks, L. A. *Angew. Chem. Int. Ed.* **2012**, *51*, 3410-3413; (d) Sedai, B.; Baker, R. T. *Adv. Synth. Catal.* **2014**, *356*, 3563-3574; (e) Gao, Y. J.; Zhang, J. G.; Chen, X.; Ma, D.; Yan, N. *ChemPluschem* **2014**, *79*, 825-834; (f) Dawange, M.; Galkin, M. V.; Samec, J. S. M. *ChemCatchem* **2015**, *7*, 401-404; (g) Vardon, D. R.; Franden, M. A.; Johnson, C. W.; Karp, E. M.; Guarnieri, M. T.; Linger, J. G.; Salm, M. J.; Strathmann, T. J.; Beckham, G. T. *Energy Environ. Sci.* **2015**, *8*, 617-628; (h) Ma, Y. Y.; Du, Z. T.; Liu, J. X.; Xia, F.; Xu, J. *Green Chem.* **2015**, *17*, 4968-4973; (i) Deng, W.; Zhang, H.; Wu, X.; Li, R.; Zhang, Q.; Wang, Y. *Green Chem.* **2015**, *17*, 5009-5018; (j) Wang, M.; Lu, J. M.; Zhang, X. C.; Li, L. H.; Li, H. J.; Luo, N. C.; Wang, F. *ACS Catal.* **2016**, *6*, 6086-6090; (k) Luo, N.; Wang, M.; Li, H.; Zhang, J.; Liu, H.; Wang, F. *ACS Catal.* **2016**, 7716-7721.

(11) (a) Sturgeon, M. R.; Kim, S.; Lawrence, K.; Paton, R. S.; Chmely, S. C.; Nimlos, M.; Foust, T. D.; Beckham, G. T. *ACS Sustainable Chem. Eng.* **2014**, *2*, 472-485; (b) Jia, S.; Cox, B. J.; Guo, X.; Zhang, Z. C.; Ekerdt, J. G. *ChemSusChem* **2010**, *3*, 1078-1084; (c) Scott, M.; Deuss, P. J.; de Vries, J. G.; Prechtl, M. H. G.; Barta, K. *Catal. Sci. Technol.* **2016**, *6*, 1882-1891.

(12) (a) Jia, S.; Cox, B. J.; Guo, X.; Zhang, Z. C.; Ekerdt, J. G. *Holzforschung* **2010**, *64*, 577-580; (b) Katahira, R.; Mittal, A.; McKinney, K.; Chen, X.; Tucker, M. P.; Johnson, D. K.; Beckham, G. T. *ACS Sustainable Chem. Eng.* **2016**, *4*, 1474-1486.

(13) (a) Song, Q.; Wang, F.; Cai, J.; Wang, Y.; Zhang, J.; Yu, W.; Xu, J. *Energy Environ. Sci.* **2013**, *6*, 994-1007; (b) Ma, R.; Hao, W.; Ma, X.; Tian, Y.; Li, Y. *Angew. Chem. Int. Ed.* **2014**, *53*, 7310-7315.

(14) (a) Son, S.; Toste, F. D. *Angew. Chem. Int. Ed.* **2010**, *49*, 3791-3794; (b) Harms, R. G.; Markovits, II; Drees, M.; Herrmann, H. C.; Cokoja, M.; Kuhn, F. E. *ChemSusChem* **2014**, *7*, 429-434; (c) Haibach, M. C.; Lease, N.; Goldman, A. S. *Angew. Chem. Int. Ed.* **2014**, *53*, 10160-10163; (d) Zhou, X.; Mitra, J.; Rauchfuss, T. B. *ChemSusChem* **2014**, *7*, 1623-1626; (e) Galkin, M. V.; Dahlstrand, C.; Samec, J. S. M. *ChemSusChem* **2015**, *8*, 2187-2192.

(15) Kim, S.; Chmely, S. C.; Nimos, M. R.; Bomble, Y. J.; Foust, T. D.; Paton, R. S.; Beckham, G. T. *J. Phys. Chem. Lett.* **2011**, *2*, 2846-2852.

(16) Rahimi, A.; Azarpira, A.; Kim, H.; Ralph, J.; Stahl, S. S. *J. Am. Chem. Soc.* **2013**, *135*, 6415-6418.

(17) Nguyen, J. D.; Matsuura, B. S.; Stephenson, C. R. *J. Am. Chem. Soc.* **2014**, *136*, 1218-1221.

(18) Strassberger, Z.; Alberts, A. H.; Louwerse, M. J.; Tanase, S.; Rothenberg, G. *Green Chem.* **2013**, *15*, 768-774.

(19) Wang, L. L.; Zhu, Y. C.; Li, H. B.; Li, Q. W.; Qian, Y. T. *J. Solid State Chem.* **2010**, *183*, 223-227.

(20) (a) Kresse, G.; Hafner, J. *Phys. Rev. B* **1993**, *47*, 558-561; (b) Kresse, G.; Furthmuller, J. *Comp. Mater. Sci.* **1996**, *6*, 15-50.

(21) Kresse, G.; Joubert, D. *Phys. Rev. B* **1999**, *59*, 1758-1775.

(22) (a) Perdew, J. P.; Yue, W. *Phys. Rev. B* **1986**, *33*, 8800-8802; (b) Perdew, J. P.; Wang, Y. *Phys. Rev. B* **1992**, *45*, 13244-13249.

(23) Grimme, S.; Antony, J.; Ehrlich, S.; Krieg, H. *J. Chem. Phys.* **2010**, *132*, 154104.

(24) Lu, J.; Wang, M.; Zhang, X.; Heyden, A.; Wang, F. *ACS Catal.* **2016**, *6*, 5589-5598.

(25) (a) Whiffen, V. M. L.; Smith, K. J. *Energy Fuel* **2010**, *24*, 4728-4737; (b) Jongerius, A. L.; Jastrzebski, R.; Bruijnincx, P. C. A.; Weckhuysen, B. M. *J. Catal.* **2012**, *285*, 315-323.

(26) (a) Kumar, C. R.; Anand, N.; Kloekhorst, A.; Cannilla, C.; Bonura, G.; Frusteri, F.; Barta, K.; Heeres, H. J. *Green Chem.* **2015**, *17*, 4921-4930; (b) Narani, A.; Chowdari, R. K.; Cannilla, C.; Bonura, G.; Frusteri, F.; Heeres, H. J.; Barta, K. *Green Chem.* **2015**, *17*, 5046-5057.

(27) (a) Yang, G. Y.; Ma, Y. F.; Xu, J. *J. Am. Chem. Soc.* **2004**, *126*, 10542-10543; (b) Zhang, W.; Ma, H.; Zhou, L.; Miao, H.; Xu, J. *Chin. J. Catal.* **2009**, *30*, 86-88; (c) Yang, X.; Wang, Y.; Zhou, L.; Chen, C.; Zhang, W.; Xu, J. *J. Chem. Technol. Biotechnol.* **2010**, *85*, 564-568; (d) Zhou, L.; Zhang, C.; Fang, T.; Zhang, B.; Wang, Y.; Yang, X.; Zhang, W.; Xu, J. *Chin. J. Catal.* **2011**, *32*, 118-122; (e) Yang, X.; Wang, Y.; Zhang, C.; Fang, T.; Zhou, L.; Zhang, W.; Xu, J. *J. Phys. Org. Chem.* **2011**, *24*, 693-697.

(28) (a) Srifa, P.; Galkin, M. V.; Samec, J. S. M.; Hermansson, K.; Broqvist, P. *J. Phys. Chem. C* **2016**, *120*, 23469-23479; (b) Bernt, C. M.; Bottari, G.; Barrett, J. A.; Scott, S. L.; Barta, K.; Ford, P. C. *Catal. Sci. Technol.* **2016**, *6*, 2984-2994.

(29) Drescher, T.; Niefind, F.; Bensch, W.; Grunert, W. *J. Am. Chem. Soc.* **2012**, *134*, 18896-18899.

(30) Van den Bosch, S.; Schutyser, W.; Vanholme, R.; Driessen, T.; Koelewijn, S. F.; Renders, T.; De Meester, B.; Huijgen, W. J. J.; Dehaen, W.; Courtin, C. M.; Lagrain, B.; Boerjan, W.; Sels, B. F. *Energy Environ. Sci.* **2015**, *8*, 1748-1763.